Separation Science and Technology
Publication details, including instructions for authors and subscription information:
http://www.informaworld.com/smpp/title~content=t713708471

Electrostatic Collection Efficiency in Binary Fluidized Beds

A. Romero[a]; J. Guardiola[a]; J. Rincon[a]
[a] DEPARTMENT OF CHEMICAL ENGINEERING, UNIVERSITY OF ALCALá DE HENARES, MADRID, SPAIN

To cite this Article Romero, A. , Guardiola, J. and Rincon, J.(1992) 'Electrostatic Collection Efficiency in Binary Fluidized Beds', Separation Science and Technology, 27: 1, 87 — 103
To link to this Article: DOI: 10.1080/01496399208018867
URL: http://dx.doi.org/10.1080/01496399208018867

SEPARATION SCIENCE AND TECHNOLOGY, 27(1), pp. 87–103, 1992

Electrostatic Collection Efficiency in Binary Fluidized Beds

A. ROMERO, J. GUARDIOLA, and J. RINCON
DEPARTMENT OF CHEMICAL ENGINEERING
UNIVERSITY OF ALCALÁ DE HENARES
MADRID, SPAIN

Abstract

Fluidized beds of binary mixtures have been used to clean air streams containing dust particles in the size range 4.4 to 14 μm. All beds were composed of glass beads and plastic granules mixed at different proportions. The effect on the electrostatic collection efficiency of a number of variables, including type of collecting mixture, bed height, and gas velocity, was examined. To calculate the single collection efficiency from experimental results, an early model proposed by Clift et al. was used. The electrostatic collection efficiency was determined by subtracting the other individual mechanism efficiencies from the single particle collection efficiency.

INTRODUCTION

The use of fluidized bed filters for removing fine particles from gaseous streams is a widely applied engineering practice. After the pioneering work of Meissner and Mickley (*2*), a number of investigations have been conducted to characterize the behavior of fluidized beds (*3–6*). More recently the application of external forces—either electric or magnetic—to enhance filtration has also been explored (*7–11*).

Another method for improving filtration efficiency is to boost electrostatic charge generation. In a fluidization process—because of its own nature—the electrostatic charging of the bed dielectric granules due to the mutual friction between the granules and between the granules and the container wall is almost unavoidable. This phenomenon, called triboelectrification, may be effective either in increasing the efficiency of aerosol collection by collision or subsequent to collision it may assist adhesion between aerosol and collector (*5*, *12*, *13*).

The amount of charge generated depends on numerous variables. Among others, the following may be mentioned: bulk chemical composition, size and shape of the bodies brought into contact, state of their surfaces, temperature, humidity, type of contact (touching, impacting, rubbing), and area and duration of contact. The large list of relevant variables may be one of the reasons for both the known difficulty in reproducing triboelectric experiments and the shortage of papers on static electrification.

The mechanisms by which charge is generated have been explained in terms of electron exchange (*14*) and are not described here. However, it should be remarked that the charge generated may be higher when the bodies brought into contact have different dielectric constants and high surface resistivity. Experimental results by Gradon (*15*) with fabric filters confirm this statement. He found the filtration efficiency to be higher when, instead of homogeneous fibers, a mixture of them with different dielectric constants ($\epsilon_1 = 1.2$, $\epsilon_2 = 9.0$) and high surface resistivity made up the filter bed. To the knowledge of the authors, no experimental work of this nature (involving binary mixtures of insulating materials) has been undertaken with fluidized beds.

The aim of the present work was to conduct a systematic experimental study of aerosol filtration in binary fluidized beds (BFB) of insulating materials, and to examine the effect of various operating variables on the electrostatic collection efficiency. The experimental results on particle collection were analyzed on the basis of single particle collection efficiency. This variable was calculated from a widely applied model (*13*, *16*, *17*) proposed by Clift et al. (*1*). The electrostatic collection efficiency was determined by subtracting the other individual mechanism efficiencies from the single particle collection efficiency.

EXPERIMENTAL

Apparatus and Materials

The aerosol particles were carbon fines, a dark powder with a low cohesiveness in which the carbon content is about 80%, with fly ash making up the balance. The bed particles were mixtures of five different size fractions of glass beads and a one size fraction of plastic spherical particles. Table 1 lists the relevant properties of both collector and aerosol particles.

The basic experimental facility used in this work is shown schematically in Fig. 1 and consists of the following:

1. *BFB Filter*. The BFB filter itself consists of a binary mixture of plastic and glass spherical particles supported by a flat plate distributor ($A_L = 4.5\%$, $d_0 = 1.5$ mm) inside a perspex column 9 cm in diameter

TABLE 1
Powder Characterization

Material	Key	Average diameter (μm)	Density (kg/m³)	Group of Geldart	u_{mf} (m/s)
Plastic	PP	3100	980	D	0.86
Glass	G1	1090	2700	D	0.62
Glass	G2	775	2700	D	0.42
Glass	G3	655	2700	D	0.36
Glass	G4	550	2700	B	0.26
Glass	G5	460	2700	B	0.19
Carbon	—	4.4–14.0	1850	—	—

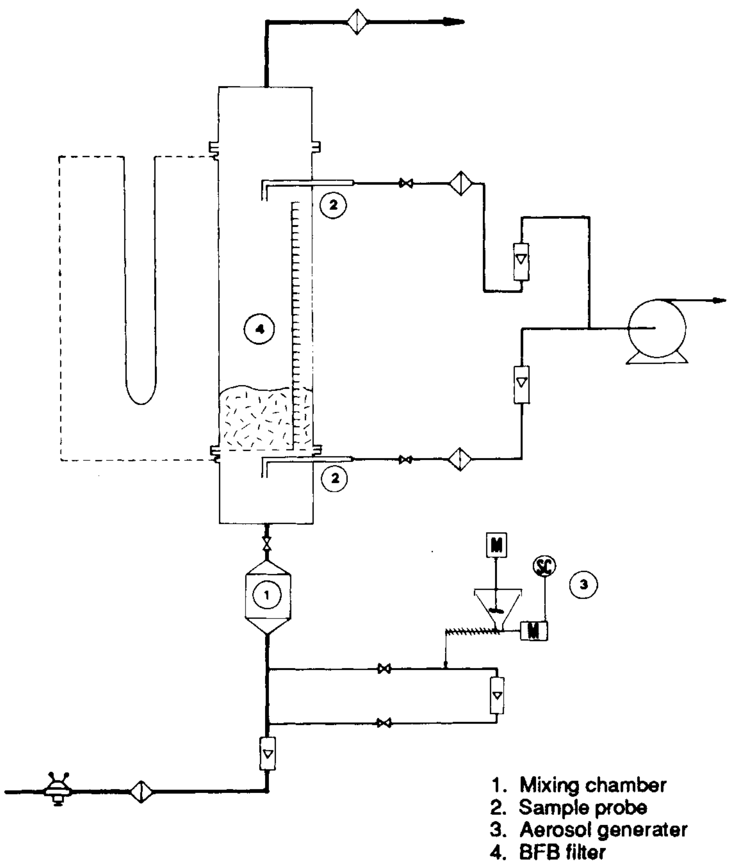

FIG. 1. Experimental facility.

and 90 cm in length. This section was attached at both ends to two perspex tubes with the same internal diameter and 20 cm in length each. In these perspex sections were attached the sampling probes and pressure taps.

2. *Aerosol Generating System.* The aerosol generator consists of a fluidized bed of glass ballotini into which a mixture of carbon fines and ballotini is fed through a rotating brush screw. Once fluidized, the fines are elutriated with air and passed through a settling chamber which removes the larger particles. The dust load can be varied by varying either the screw speed or the proportions of fines in the mixture.

   The air stream supplied by the compressor was divided into two parts. One of them was used to operate the aerosol generator. The exit air stream from the aerosol generator was then combined with the rest of the air at the mixing chamber. The gas stream from this chamber was finally supplied to the BFB filter.
3. *Sampling System.* The influent and effluent aerosol concentrations were determined by sampling the loaded air before and after the filter. Once the gas was collected in a membrane filter, it was then transported to a desiccator and the concentration and particle size were analyzed in an electronic particle counter (Coulter Counter, model ZM).

Procedure

Prior to each experiment, the glass and plastic particles that made up the bed were cleaned with water, dried, and mixed in the proportions required for each experiment; then they were introduced into the column. Next the air supply was switched on.

After completing these steps, the aerosol generator was started and the aerosol suspension, after being mixed with the rest of the air in the mixing chamber, was allowed to pass through the filter bed. Aerosol samples were simultaneously taken isokinetically at both the inlet and the exit of the filter. Each experiment lasted 20 min.

Experimental Variables

The experimental variables considered in this work are the following: gas velocity, bed height (expressed in terms of the equivalent fixed-bed height), aerosol size, and type of collecting mixture. Table 2 shows the collecting mixtures (plastic and glass particles mixed at different proportions) used in this work. Each collecting mixture is named by M with a superscript and a subscript. The subscript refers to the size of the glass

TABLE 2
Types of Collecting Mixtures

	d_p (glass), μm				
x_v' (%)	1090	775	655	550	460
70	M_1^{70}	M_2^{70}	M_3^{70}	M_4^{70}	M_5^{70}
50	M_1^{50}	M_2^{50}	M_3^{50}	M_4^{50}	M_5^{50}
30	M_1^{30}	M_2^{30}	M_3^{30}	M_4^{30}	M_5^{30}

used in the mixture, and the superscript refers to the volumetric proportion of glass in it. For example M_2^{30} refers to a plastic and glass particle mixture where the average size of glass (G2) is 775 μm and its volumetric proportion is 30%. Table 3 shows the more significant properties of these mixtures.

A summary of the experimental conditions is given in Table 4. The data are tabulated in Reference *17*.

TABLE 3
Characteristics of Collecting Mixtures

Mixture	ρ_M (kg/m^3)	d_M (μm)	u_{mf} (m/s)
M_1^{70}	2161	1367	0.58
M_1^{50}	1812	1638	0.57
M_1^{30}	1472	2028	0.68
M_2^{70}	2161	1012	0.37
M_2^{50}	1812	1264	0.41
M_2^{30}	1472	1667	0.45
M_3^{70}	2161	869	0.33
M_3^{50}	1812	1104	0.44
M_3^{30}	1472	1498	0.41
M_4^{70}	2161	740	0.27
M_4^{50}	1812	955	0.32
M_4^{30}	1472	1331	0.38
M_5^{70}	2161	627	0.19
M_5^{50}	1812	820	0.23
M_5^{30}	1472	1172	0.28

TABLE 4
Experimental Variables

u_f (m/s)	0.50	0.75	1.00
H_f (cm)	5.5	11.0	16.5
d_a (μm)	From 4.4 to 14		
Mixture	As defined in Table 2		

RESULTS AND DISCUSSION

Data Treatment

The performance of a fluidized bed filter can be described by its overall penetration, P, defined as

$$P = c_e/c_i \quad (1)$$

where c_i and c_e are the particle concentrations of the influent and effluent streams, respectively.

The overall penetration provides a direct indication of particulate removal capability. However, the quantity found to be useful in characterizing the particle collection capability is the so-called single particle collection efficiency, E. The reason for this is that E can be readily correlated with the operating variables.

To calculate the single particle collection efficiency, it is usually assumed that the various separate efficiencies are additive (*18*). These efficiencies correspond to each individual process causing filtration (diffusion, inertia, interception, gravity, and electrostatic). In this paper, all these mechanisms will be taken into account.

The purpose of the present work is to show the effect of various operating variables on the electrostatic collection efficiency E_E. E_E can be estimated from experimental measurements of penetration if previously a macroscopic fluidized bed filter model is used to obtain the individual collection efficiency E. Then, because the efficiencies are considered additive, E_E can be determined by subtracting the efficiencies corresponding to the other individual collection mechanisms from the individual collection efficiency, E. The expressions listed in Table 5 may be used to calculate the collection efficiencies due to inertia, diffusion, gravity, and interception. Figure 2 shows the aforementioned calculus sequence for E_E.

The fluidized-bed filter model used to interpret the experimental results was first proposed by Clift et al. (*1*). It is a bubbling bed model of filtration that considers the bed to consist of two regions: the jetting region, just above the distributor, and the bubbling region, higher up in the bed.

TABLE 5
Correlations to Calculate the Individual Collection Efficiency Due to Each Filtration Mechanism

Mechanism	Correlation	Remarks	Author
Inertial impaction	$St > 1.214$ $E_I = \left[1 + \frac{0.75 \ln (2St)}{St - 1.214}\right]^{-2} \tau f(\epsilon)$	The adhesion probability parameter, τ (Yoshida and Tien, 1985), has been introduced to take into account the possible rebound effect: $\tau = 0.00318St^{-1.248}$	Langmuir, 1948 (*28*)
	$1.214 > St > 0.083$ $E_I = \left[\frac{St}{St + 0.5}\right]^2 \tau f(\epsilon)$	The porosity effect has been considered through the correction factor proposed by Wilson and Geoankopolis, 1966 (*30*): $f(\epsilon) = 1.09/\epsilon$	
Brownian diffusion	$E_D = \frac{4Sh}{Pe} f(\epsilon)$	$Sh = 0.997Pe^{1/3}$, Levich, 1962 (*29*) $f(\epsilon) = 1.09/\epsilon$	Wilson and Geoankopolis, 1966 (*30*)
Direct interception	$E_{DI} = 1.5 \left[\frac{d_a}{d_M}\right]^2 f^3(\epsilon)$	$f(\epsilon) = 1.09/\epsilon$	Gutfinger and Tardos, 1979 (*5*)
Gravity	$E_G = 0.0375 \left[\frac{u_t}{u_f}\right]^{1/2}$		Paretsky, 1972 (*31*)

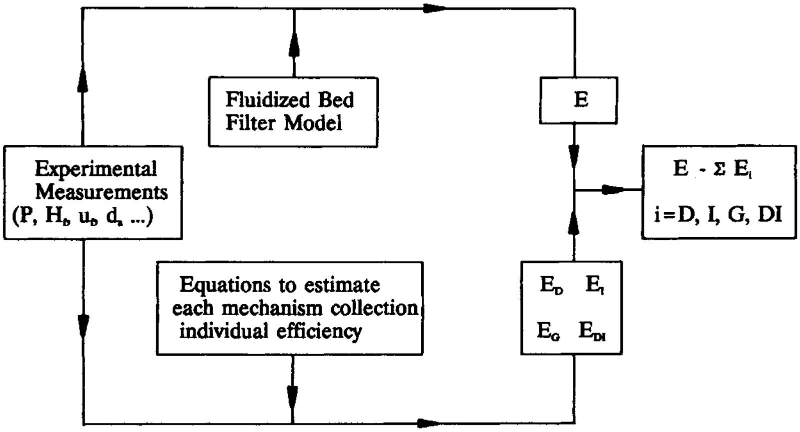

FIG. 2. Calculus sequence scheme for E_F.

Although more sophisticated models have been proposed (*19*, *20*), the Clift model has been used because it yields results in good agreement with experiments (*13*, *16*).

According to the model of Clift et al. (*1*), filtration may occur either in a fully mixed particulate phase or with plug flow in such a phase. However, for the velocity range in which fluidized beds operate, it may be supposed that filtration occurs with plug flow (*1*) and, therefore, that penetration may be obtained from the following expression:

$$P = \frac{X(m_2 e^{-m1} - m_1 e^{-m2}) - (1 - \beta)m_1 m_2(e^{-m1} - e^{-m2})}{X(m_2 - m_1)} \tag{2}$$

where m_1 and m_2 are the square roots of the equation

$$(1 - \beta)m^2 - [X + (1 - \beta)k]m + kX(1 - \beta e^{-Y}) = 0 \tag{3}$$

In accordance with Expressions (2) and (3), the overall penetration is calculated as a function of four parameters (X, β, k, Y) which are defined in the Notation Section. The X parameter is estimated from the correlation due to Darton (*21*):

$$X = \frac{67.4 u_{mf}}{(u_f - u_{mf})^{0.6} g^{0.2} A_0^{0.1}} \left[1 - \left(\frac{4\sqrt{A_0}}{H_f + 4\sqrt{A_0}}\right)\right]^{0.2} \tag{4}$$

The model, initially developed for monocomponent beds (the particles in the bed are uniform in size and density), can be applied to binary beds if, for the particle mixture making up the bed, an average density, ρ_M, and diameter, d_M, are introduced. In this work they are defined as follows:

$$\rho_M = \frac{\rho_F \rho_P}{x_F \rho_P + x_P \rho_F} \tag{5}$$

$$d_M = \frac{x_F \rho_P + x_P \rho_F}{x_F \rho_P d_P + x_P \rho_F d_F} d_F d_P \tag{6}$$

where the subscripts F and P refers to the flotsam and jetsam components, respectively. x_F and x_P are their weight fractions in the mixture.

Expression (2) quantifies the penetration in the bubbling region of a fluidized bed. However, if it is assumed that the filter consists of a single bubble region, it can be applied to the whole bed. In this paper we make such an assumption and use Expression (2) to evaluate the single collection efficiency, E, from the experimental value of the overall penetration, P. Although it is a simplification, the data are not considered accurate enough, especially at higher values of P, to be worthy of more sophisticated treatment.

Effect of Collecting Mixture

The influence of the collecting mixture on the electrostatic collection efficiency, E_E, has been studied through both the size of the glass used in the mixture and its volumetric proportion in it.

In relation to the glass size effect, Fig. 3 shows—for three different proportions of glass in the mixture—that the smaller the glass particle diameter, the greater the electrostatic collection becomes. This can be explained in terms of the total particle surface available for rubbing in the fluidized bed. Since this surface is larger for the smallest particles, it could be expected that the amount of charge generated is greater in this case and, therefore, the electrostatic collection efficiency is greater.

To study the effect of the proportion of glass on the electrostatic collection efficiency, mixtures containing glass beads in volumetric percentages of 30, 50, 70, and 100 were tested. Figure 4 shows this effect when the glass used in the mixture was 550 μm in diameter. From this figure, two conclusions can be drawn:

1. Binary fluidized beds of mixed materials exhibit greater values of E_E than monocomponent fluidized beds.

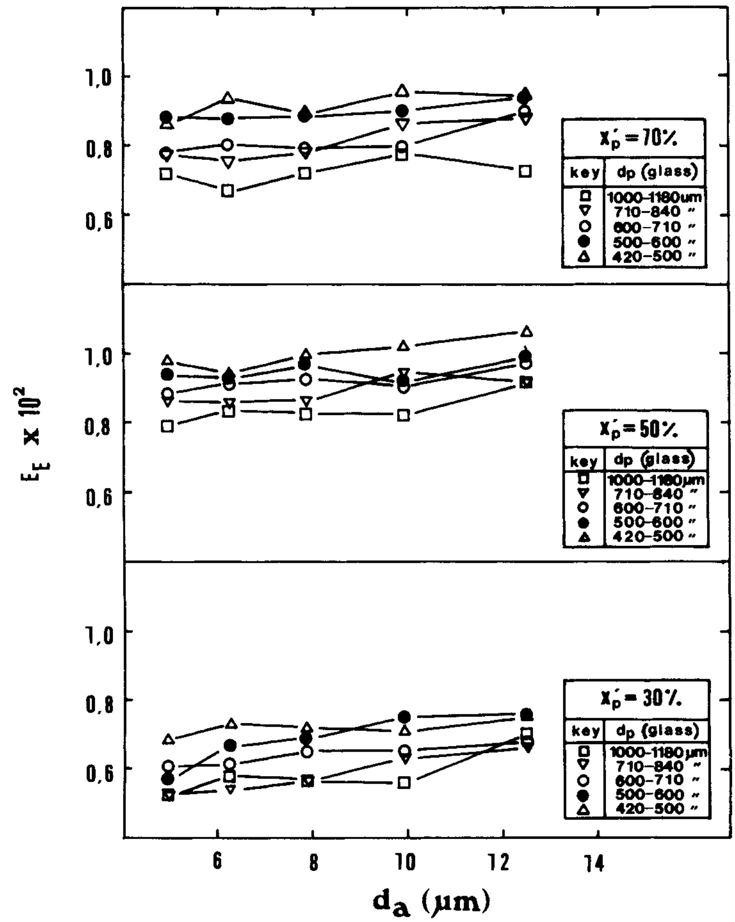

FIG. 3. Effect of glass size on the electrostatic collection efficiency (H_{mf} = 11 cm, c_i = 6.15 × 10^{-5} g/m^3).

2. The mixture with a glass volumetric proportion of 50% presents the greatest electrostatic collection efficiency. Proportions of glass above and below this figure lead to a lesser value of E_E that is the smallest one corresponding to the largest amount of glass in the mixture.

Other glass sizes (460, 655, 775, and 1090 μm average diameter) were tested and yielded similar results.

The first conclusion confirms that in fluidized beds—as expected—the charge generated is greater when the bodies brought into contact have

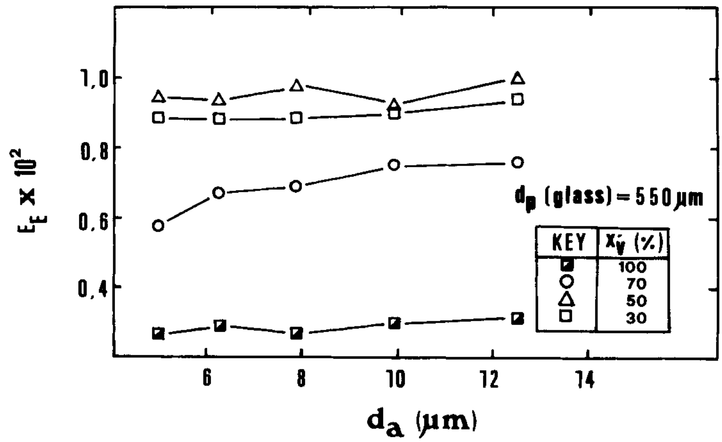

FIG. 4. Electrostatic collection efficiency for monocomponent and binary beds (u_f = 0.75 m/s, H_{mf} = 11 cm, c_i = 6.15 × 10^{-5} g/m^3).

different dielectric constants (ϵ_g = 5, ϵ_p = 2.3). In addition, it is worth noting that the electric charge can influence not only the deposition process but also the secondary release of particles.

The variation of E_E with the percentage of glass particles in the mixture seems to depend on the quality of contact, i.e., on the number of contacts between particles of different natures. This would justify the larger E_E obtained for the mixture containing a 50% volumetric proportion of glass. As for the difference between mixtures with 70 and 30% of glass particles, it can be argued that bed segregation, which is greater in the first case, could have caused the decrease in the amount of charge generated and, therefore, in E_E.

Effect of Bed Height

Figure 5 shows the results obtained in experiments with different bed heights. It can be observed that, in the range of this variable, there was no influence of bed height on the electrostatic collection efficiency.

Rojo et al. (*22*) found that for bubbling fluidization the amount of charge generated increased with bed height. However, it should be noted that an increase of bed height can also increase the rate of charge dissipation through the wall surface in contact with the bed (*13*).

The effect of this variable on the electrostatic collection efficiency can be explained by bearing in mind the results expressed above. There are two processes causing electrostatic charge to vary in a fluidized bed: charge generation and charge dissipation. If it is assumed that both processes

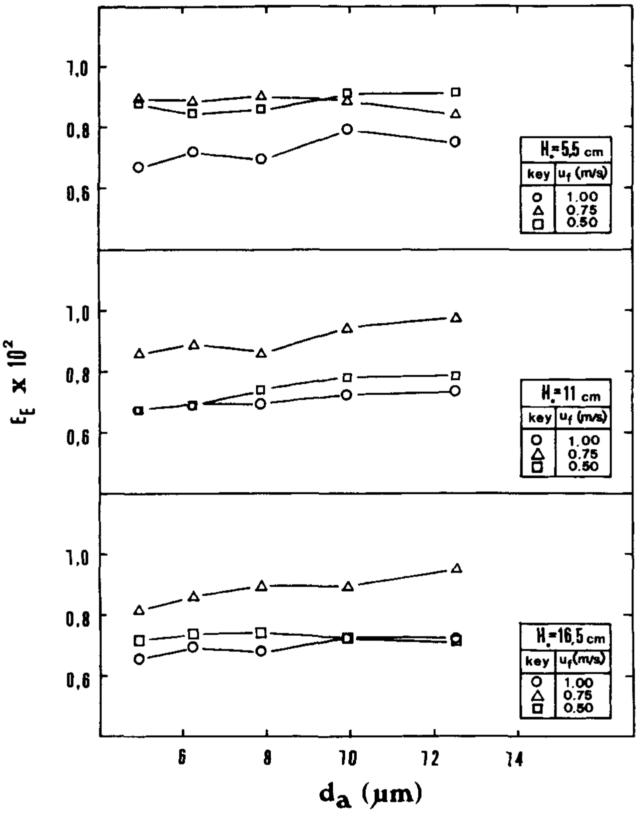

FIG. 5. Effect of bed height on the electrostatic collection efficiency (H_{mf} = 11 cm, d_M = 1331 μm, c_i = 6.15 × 10^{-5} g/m³).

increase with bed height at a similar rate, then no net effect on E_E should be found when the bed height is varied. Although this assumption agrees with experimental results, it is obvious that further experimental work is needed to confirm it quantitatively.

Effect of Gas Velocity

For gas bubbling fluidization (u_f = 0.50 and 0.75 m/s in this work), the curves plotted in Fig. 6 show that E_E increase with the gas velocity. However, if the gas velocity produces slugs (u_f = 1.00 m/s in this work), the opposite effect is observed. From these results it can be deduced that the influence of gas velocity on E_E is closely related to the type of fluidization

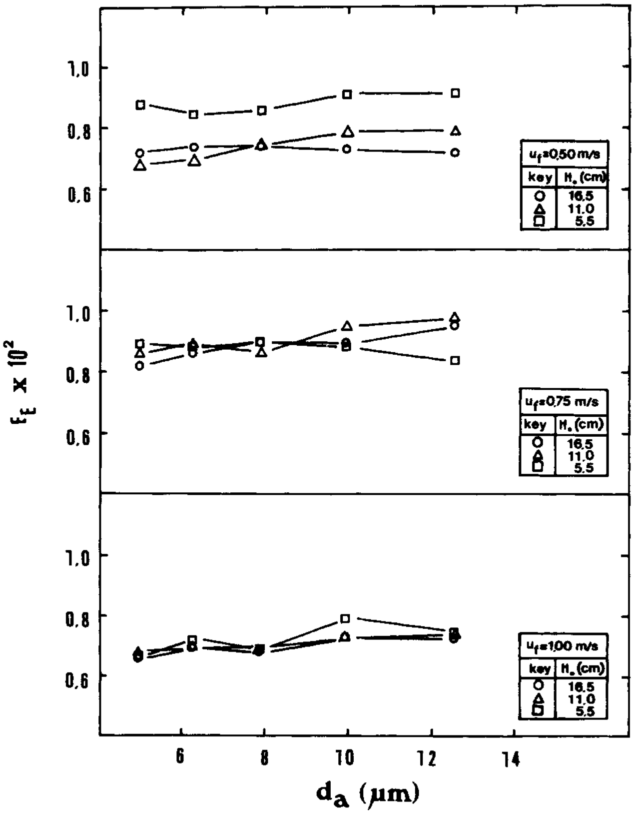

FIG. 6. Effect of gas velocity on the electrostatic collection efficiency (d_M = 1331 μm, c_i = 6.15×10^{-5} g/m^3).

(bubbling or slugging). This influence will be explained by considering the experimental work of other authors.

On the one hand, it is well known that in bubbling beds the bubbles increase their size and velocity as they rise. When the bed is deep enough, bubbles become slugs with a lower rising velocity than free bubbles of the same volume. Because bubble formation frequency at the distributor of a fluidized bed seems to be roughly constant with increasing air flow-rate, Rowe et al. (*23*) and Ho et al. (*24*) suggested that bubbles placed at a constant bed height become bigger as the gas velocity increases. On the other hand, Boland and Geldart (*25*) found that—because the higher rising velocity of bigger bubbles causes a larger motion of bed particles—the charge generated in a fluidized bed increases with bubble diameter.

Accordingly, the effect of gas velocity on E_E can be explained in the following way: For bubbling fluidization the electrostatic charge generated increases with the gas velocity. The higher velocity reached by bubbles causes an intense motion of bed particles and hence more friction. The greater level of charge will yield a greater electrostatic collection efficiency. On the contrary, for slugging fluidization, slugs that have a lower rising velocity than free bubbles will reduce particle motion and therefore the electrostatic charge generated and the electrostatic collection efficiency.

CONCLUSIONS

1. Electrostatic collection efficiency is greater when binary fluidized beds of mixed materials are used instead of unicomponent beds. The reason could be that static charge caused by triboelectrification of materials with different dielectric constants is greater than static charge originated by triboelectrification of a single material. Further work will be needed to confirm this statement.
2. The influence of collecting mixture on E_E has been studied through both glass particle size and glass particle proportion. The effects observed are: 1) E_E decreases with glass particle size because of the smaller total particle surface available for rubbing, and 2) E_E goes through a maximum for a 50% glass volumetric proportion because of a better quality of contact.
3. The effect of gas velocity on E_E is closely connected to the type of glass fluidization. For a bubbling bed, E_E increases with increasing values of u_f, while for slugging fluidization the opposite effect is observed.
4. An equality between the rates at which charge generation and charge dissipation increase with bed height is found to be responsible for why E_E is not affected by bed height.

NOTATION

A_L free area (dimensionless)
A_0 distributor plate orifice area (m^2)
c_a average concentration of aerosol (kg/m^3)
c_{eff} average effluent aerosol concentration (kg/m^3)
c_{inf} average influent aerosol concentration (kg/m^3)
D molecular or Brownian diffusivity (m^2/s)
D_c column diameter (m)
d_a aerosol diameter (μm)
d_0 orifice diameter of the distributor plate (μm)

d_p collector diameter (μm)
E single collection efficiency (dimensionless)
F slip correction factor (dimensionless)
g gravity (m/s^2)
H_f bed height (m)
H_{mf} minimum fluidization bed height (m)
h_j height of the jet region (m)
K interphase transfer coefficient per unit volume of bubble phase (s^{-1})
k mass transfer coefficient (m/s)
k filtration rate constant, $3E(1 - \epsilon_{mf})(H_f - h_j)/2d_p$ (dimensionless)
P penetration (dimensionless)
Pe Peclet number, $u_f d_p/D$ (dimensionless)
Sh Sherwood number, kd_p/D (dimensionless)
St Stokes number, $\rho_p d_a u_f/9\mu d_p$ (dimensionless)
u_f gas velocity (m/s)
u_{mf} minimum fluidization velocity (m/s)
X crossflow factor, $(H_f - h_j)K\epsilon_B/\beta u_f$ (dimensionless)
x weight fraction of a component in the mixture (dimensionless)
x' volume fraction of a component in the mixture (dimensionless)
Y group describing transfer from bubble phase to a single layer of collector, $\alpha d_p X/(H_f - h_j)$ (dimensionless)

Greek Symbols

α group describing filter bed associated with single layer of collector particles, $(\pi/6(1 - \epsilon_{mf}))^{1/3}$ (dimensionless)
β fraction of fluidizing gas passing through bed in bubble phase, $1 - (u_{mf}(1 - \epsilon_B)/u_f)$ (dimensionless)
ϵ bed porosity (dimensionless)
ϵ_B time-averaged fraction of cross-sectional area of fluidized bed occupied by bubble phase (dimensionless)
ϵ_g glass dielectric constant (F/m)
ϵ_p plastic dielectric constant (F/m)
μ gas viscosity (kg/ms)
ρ_a aerosol density (kg/m^3)
ρ_p collector density (kg/m^3)
τ adhesion probability (dimensionless)

Subscripts

a aerosol
D diffusion
DI direct interception
E electrostatic
F flotsam component
G gravity
g glass
I inertial
M mixture
mf at minimum fluidization conditions
P jetsam component
p plastic

Acknowledgment

The authors are thankful to the CAICYT for its financial support to this work through Project PA8602040C02-02.

REFERENCES

1. R. Clift, M. Ghadiri, and K. V. Thambimuthu, in *Progress in Filtration and Separation,* Elsevier, Amsterdam, 1981, p. 75.
2. H. P. Meissner and H. S. Mickley, *Ind. Eng. Chem., 41,* 1238 (1949).
3. C. H. Black and R. W. Boubel, *Ind. Eng. Chem., Process Des. Dev., 8,* 573 (1969).
4. K. Knettig and J. M. Beeckmans, *Can. J. Chem. Eng., 52,* 703 (1974).
5. C. Gutfinger and G. I. Tardos, *Atmos. Environ., 13,* 853 (1979).
6. A. W. Nienow and R. C. Killick, *AIChE Symp. Ser., 79,* 1 (1983).
7. H. Katz and J. T. Sears, *Can. J. Chem. Eng., 47,* 50 (1969).
8. K. Zahedi and J. R. Melcher, *Ind. Eng. Chem., Fundam., 16,* 248 (1977).
9. R. V. Albert and C. Tien, *AIChE J., 31,* 288 (1985).
10. M. Warrior and C. Tien, *Chem. Eng. Sci., 41,* 1711 (1986).
11. P. Geuzens and D. Thoenes, *Chem. Eng. Commun., 67,* 229 (1988).
12. G. I. Tardos, C. Gutfinger, and R. Pfeffer, *Ind. Eng. Chem., Fundam., 18,* 433 (1979).
13. V. Rojo, PhD Thesis, Universidad Complutense de Madrid, 1984.
14. D. J. Montgomery, *Solid State Phys., 9,* 139 (1959).
15. L. Gradon, *Ind. Eng. Chem. Res., 26,* 306 (1987).
16. B. K. C. Tan, PhD Thesis, Cambridge University, 1982.
17. J. Rincón, PhD Thesis, Universidad de Alcalá de Henares, 1989.
18. R. G. Dorman, in *Aerodynamic Capture of Particles,* Pergamon, London, 1960, p. 112.
19. M. H. Peters, L. S. Fan, and T. L. Sweeney, *AIChE J., 28,* 39 (1982).
20. K. Ushiki and C. Tien, *Ibid., 30,* 156 (1984).
21. R. C. Darton, *Trans. Inst. Chem. Eng., 57,* 134 (1979).
22. V. Rojo, J. Guardiola, and A. Vian, *Chem. Eng. Sci., 41,* 2171 (1986).
23. P. N. G. Rowe, M. J. McGillivary, and D. J. Cheesman, *Trans. Inst. Chem. Eng., 57,* 194 (1979).
24. T.-C. Ho, N. Yutani, L. T. Fan, and W. P. Walawender, *Can. J. Chem. Eng., 61,* 654 (1983).

25. D. Boland and D. Geldart, *Powder Technol.*, *5*, 289 (1972).
26. K. A. Nielsen and J. C. Hill, *Ind. Eng. Chem., Fundam.*, *15*, 149 (1976).
27. W. E. Ranz and J. B. Wong, *Ind. Eng. Chem.*, *44*, 1371 (1952).
28. I. Langmuir, *J. Meteorol.*, *5*, 175 (1948).
29. V. G. Levich, in *Physiochemical Hydrodynamics*, Prentice-Hall, Englewood Cliffs, New Jersey, 1962.
30. E. J. Wilson and C. J. Geoankoplis, *Ind. Eng. Chem., Fundam.*, *5*, 9 (1966).
31. L. Paretsky, PhD Thesis, City University of New York, 1972.

Received by editor February 11, 1991